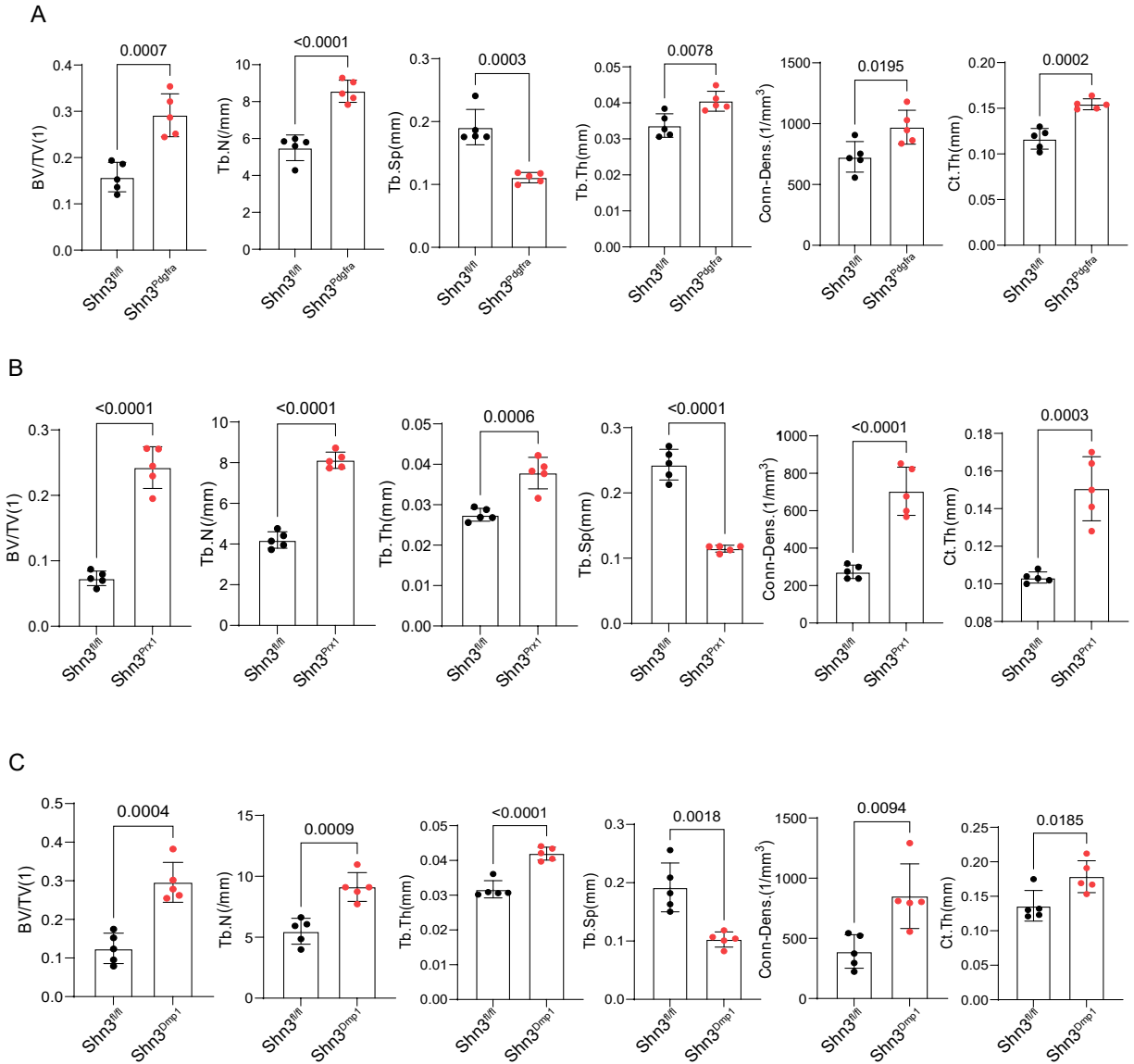# Supplemental Information

Engineering a targeted and safe

# bone anabolic gene therapy to treat

osteoporosis in alveolar bone loss

Chujiao Lin, Yeon-Suk Yang, Hong Ma, Zhihao Chen, Dong Chen, Aijaz Ahmad John, Jun Xie, Guangping Gao, and Jae-Hyuck Shim

Figure S1: Osteoblast-specific deletion of Shn3 increases bone mass in the long bones.

MicroCT analysis shows a significant increase in trabecular bone mass and cortical thickness of one-month-old $Shn3^{Pdgfr\alpha}$ (A), $Shn3^{Prx1}$ (B), $Shn3^{Dmp1}$ (C) femurs compared to $Shn3^{fl/fl}$ femurs (n = 5/group). A two-tailed unpaired Student's t-test for comparing two groups (A–C; error bars, data represent mean ± SD).
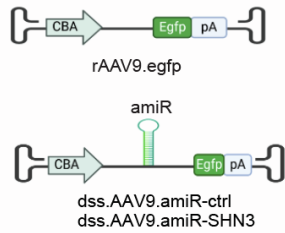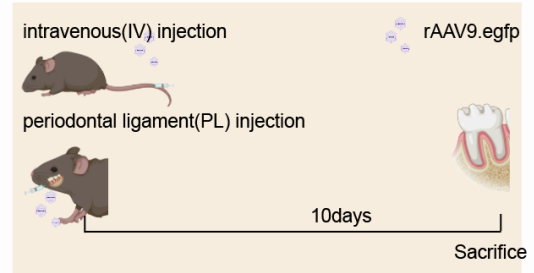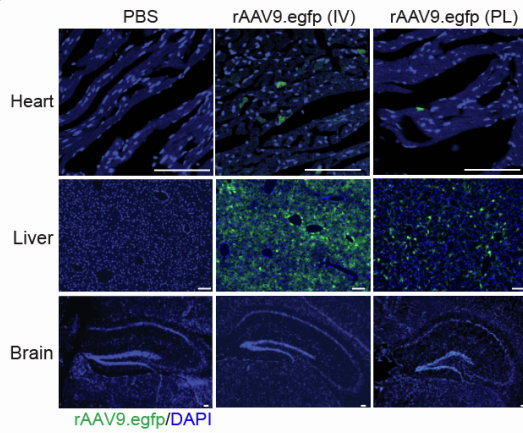
Figure S2: Biodistribution of locally or systemically injected rAAV9 in mice.

(A) The AAV vector genome containing the CMV enhancer/chicken β-actin promoter (*CBA*), an *Egfp* reporter gene (EGFP), *amiR-ctrl*, *amiR-SHN3*, *β-globin* polyA sequence (PA), and inverted terminal repeat (ITR) was packaged into rAAV9 or dss.AAV9 capsid. **(B)** Diagram of the study

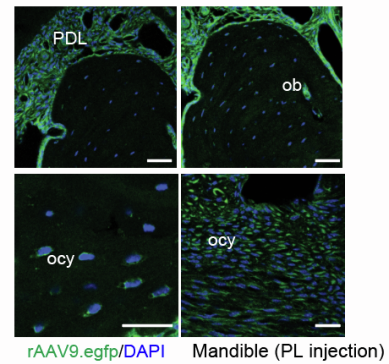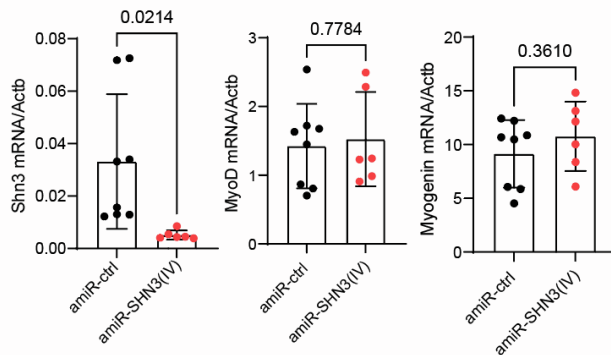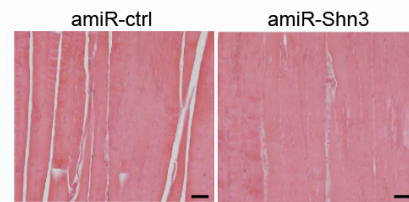and treatment methods for Figure 4A–D. 2-month-old mice were treated with EGFP-expressing rAAV9 (rAAV9.*egfp*) or dss.rAAV9 (dss.rAAV9.*egfp*) via intravenous (IV, 2.5 x 10^{13} vg/kg) injection or periodontal ligament (PL, 2.5 x 10^{12} vg/kg) injection to the mandibular first molar. 10 days later, EGFP expression in individual tissues was assessed by fluorescence microscopy in cryosectioned tissues **(C, D)**. Sham or OVX surgery was performed on 3-month-old female mice and 4 weeks later, mice were injected IV with dss.rAAV9 carrying *amiR-ctrl* or *amiR-SHN3* (2.5 x 10^{13} vg/kg). 8 weeks later, mRNA levels of *Shn3*, *MyoD*, and *Myogenin* in the skeletal muscle were measured by RT-PCR (n = 6 - 8/group, **E**). Alternatively, the skeletal muscle was stained with H&E (**F**), suggesting that SHN3 is dispensable of muscle homeostasis. PDL: periodontal ligament, ob: osteoblast, ocy: osteocyte. Scale bar, 100 μm, C, F; 50 μm, D. Ordinary one-way ANOVA with Dunnett's multiple comparisons test (**E**; data represent mean ± SD). Representative images of three replicates are displayed **(C, D, F)**.
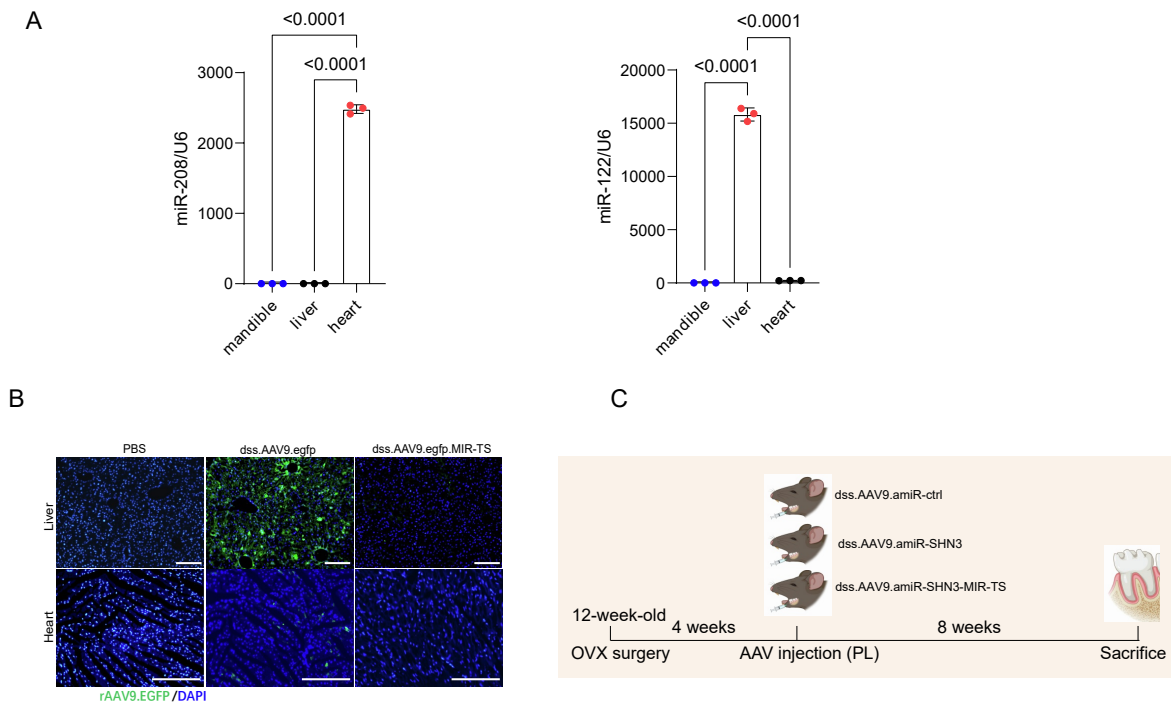
Figure S3: Characterization of the liver/heart-detargeting AAV.

(A) Expression of heart-abundant miR-208a and liver-abundant miR-122 in the mandible, liver, and heart was measured by RT-PCR analysis (n =3/group). **(B)** 2-month-old mice were injected IV with PBS, dss.AAV9.*egfp*, or dss.rAAV9.*egfp.MIR-TS* (2.5 x 10^{13} vg/kg) and ten days later, EGFP expression in the liver and heart was assessed by fluorescence microscopy (n = 3/group, scale bar: 200 μm). **(C)** Diagram of the study and treatment methods for Figure 5G-K. Sham or ovariectomy (OVX) surgery was performed on 3-month-old female mice, and four weeks later, mice were treated with PBS or dss.rAAV9 carrying *egfp*, *amiR-ctrl*, *amiR-SHN3,* or *amiR-SHN3-MIR-TS* (2.5 x 10^{12} vg/kg) via PL injection. Eight weeks after injection, *egfp* and *Shn3* expression and alveolar bone mass were assessed (n = 5/group). Ordinary one-way ANOVA with Dunnett's multiple comparisons test (**A**; data represent mean ± SD). Representative images of three replicates are displayed **(B)**.
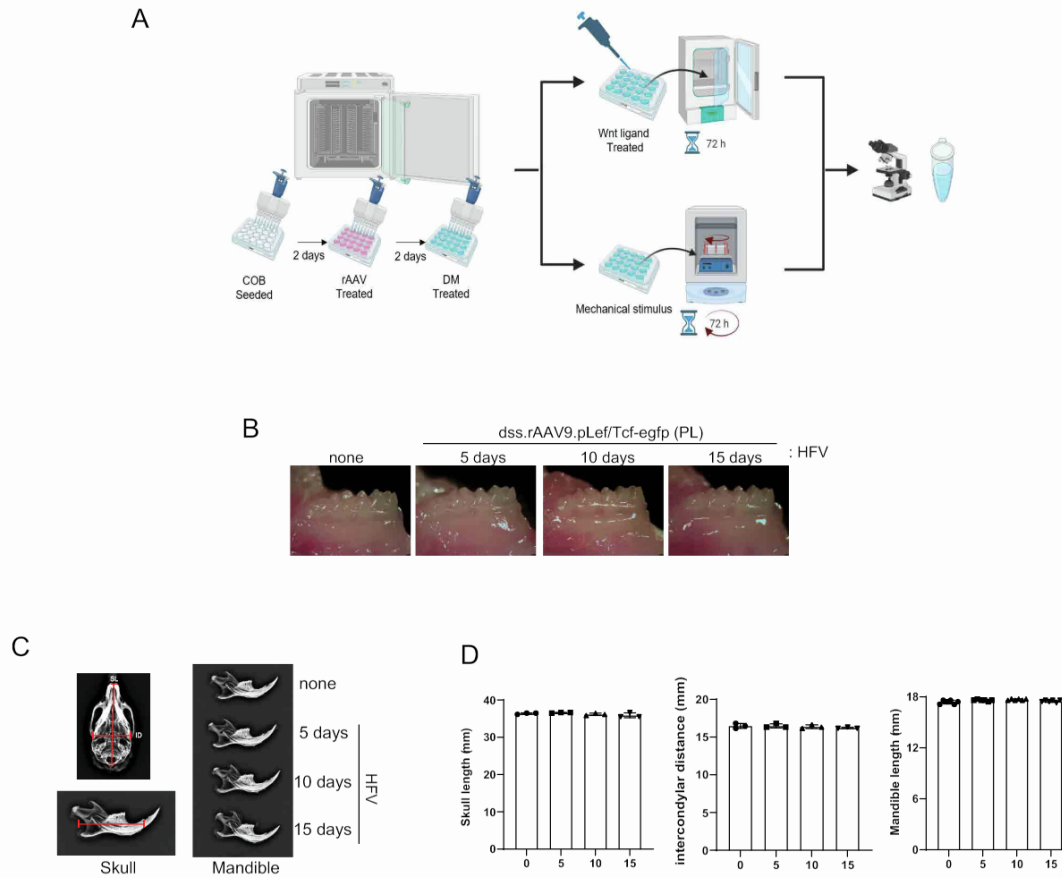
Figure S4: Vibration treatment does not affect the skull, mandible, and tooth structure.

(A) Diagram of the study and treatment methods. Calvarial osteoblasts (COB) were incubated for two days and then transduced with dss.rAAV9.pLef/Tcf-*egfp* (4 x 10^6 vg/cell) for two days and cultured in osteoblast differentiation medium (DM) for two days. AAV-treated cells were stimulated with recombinant WNT3a or flow stress for 72 hours. EGFP expression was assessed by fluorescence microscopy and RT-PCR. **(B-D)** 2-month-old mice were treated with dss.rAAV9.pLef/Tcf-*egfp* (2.5 x 10^{12} vg/kg) via PL injection into the mandibular first molar and two days later, the mandible was stimulated daily with high-frequency vibration (HFV) for up to fifteen days. Representative photographs show that the molar structure of AAV-treated mandibles is grossly normal **(B)**. Representative 2D microCT images and relative quantification show little to no effects of high-frequency vibration (HFV) treatment on skull length, intercondylar distance,

and mandible length **(C, D).** Ordinary one-way ANOVA with Dunnett's multiple comparisons test

(**D**; data represent mean ± SD). Representative images of three replicates are displayed **(B, C)**.
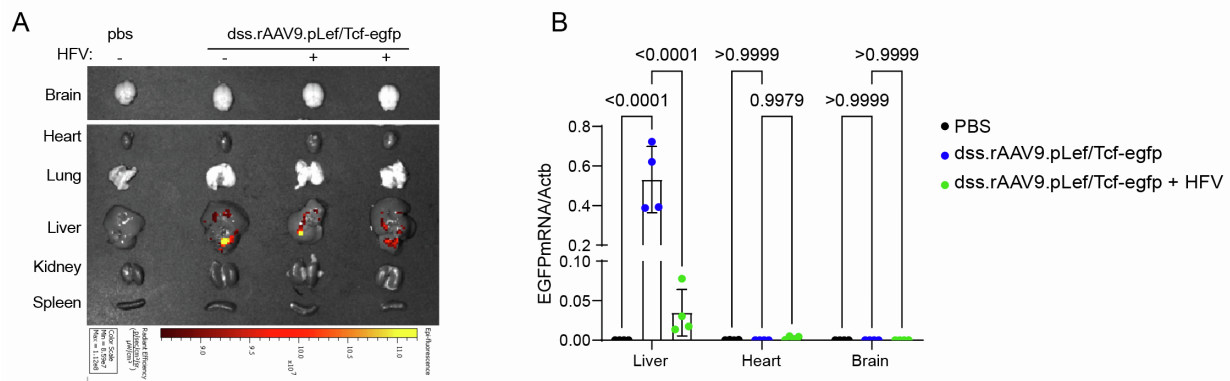
Figure S5: Effects of HFV treatment on AAV's biodistribution in mice.

2-month-old mice were treated with dss.rAAV9.pLef/Tcf-*egfp* (2.5×10^{12} vg/kg) via PL injection into the mandibular first molar and two days later, the mandible was stimulated daily with HFV treatment for 10 days. EGFP expression in individual tissues was assessed by IVIS optical imaging system **(A)** and RT-PCR **(**n = 4/group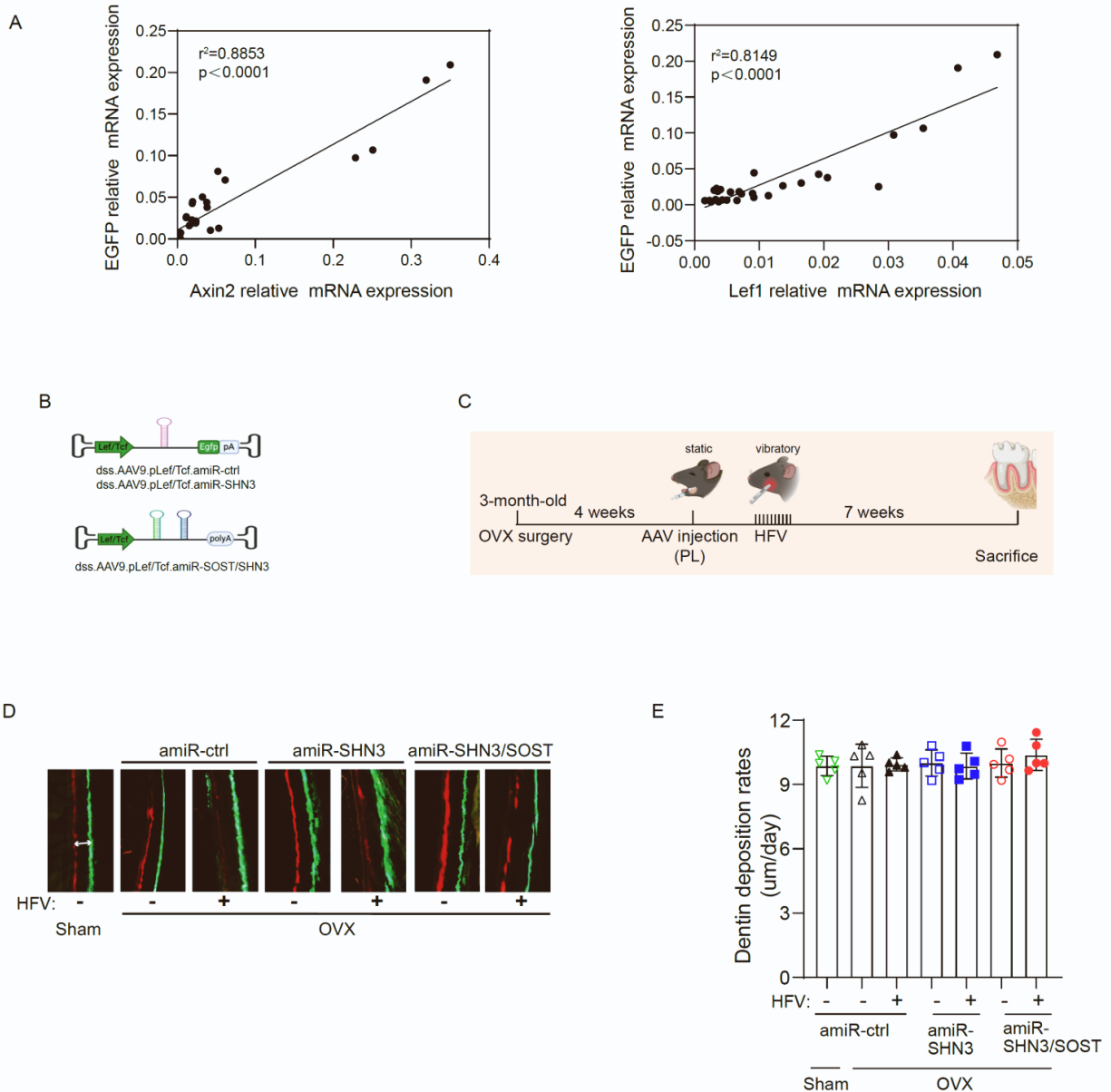, **B)**. Ordinary one-way ANOVA with Dunnett's multiple comparisons test **(B**; data represent mean ± SD). Representative images of three replicates are displayed **(A)**.

Figure S6. Vibration-inducible AAV-mediated silencing of SHN3 or SHN3/SOST does not affect tooth dentin formation in osteoporotic mice.

(A) Correlation analysis of mRNA expression of *egfp* and WNT-responsive genes, *Axin2* and *Lef1*. The experiments were performed in Figure 6E. **(B)** Diagram of the mechanical stress-responsive AAV containing *amiR-ctrl, amiR-SHN3,* or *amiR-SHN3/SOST*. The CBA promoter was replaced with the LEF/TCF promoter (pLef/Tcf). **(C)** Diagram of the study and treatment methods for

Figure 7. Sham or OVX surgery was performed on 3-month-old female mice and four weeks later, mice were treated with dss.rAAV9.pLef/Tcf carrying *amiR-ctrl*, *amiR-SHN3*, or *amiR-SOST/SHN3* (2.5 x 10^{12} vg/kg) via PL injection to the mandibular first molar. Two days later, AAV-treated mandibles were stimulated daily with HFV for ten days. Seven weeks later, mice were treated with calcein and alizarin red via intraperitoneal injection at six-day intervals and then euthanized. (D) Representative calcein/alizarin red labeling images and relative histomorphometric quantification of dentin deposition rates in the mandibular incisor are displayed **(E)**. Ordinary one-way ANOVA with Dunnett's multiple comparisons test (E, F; data represent mean ± SD). Representative images of five replicates are displayed **(D)**.

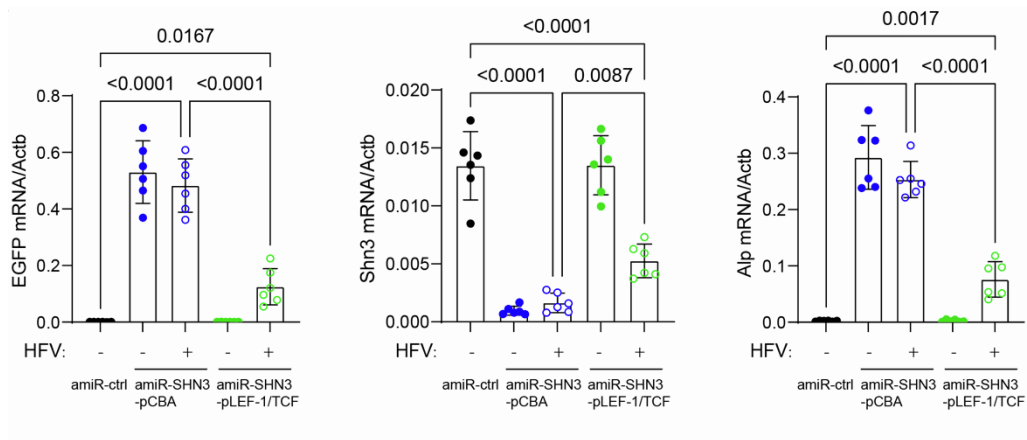**Figure S7. Comparison between constitutive and vibration-inducible silencing efficiency of *Shn3* in alveolar bone using the CBA and pLEF-1/TCF promoter, respectively.**

2-month-old mice were treated with dss.rAAV9.pCBA carrying *amiR-ctrl* or *amiR-SHN3* or dss.rAAV9.pLef/Tcf carrying *amiR-SHN3* (2.5×10^{12} vg/kg) via PL injection into the mandibular first molar and two days later, the mandible was stimulated daily with HFV treatment for 10 days. *Egfp*, *Shn3* and *Alp* mRNA expression was measured by RT-PCR (n = 5–7/group). Ordinary one-way ANOVA with Dunnett's multiple comparisons test (data represent mean ± SD).

Table S1: Sequences of primers and plasmids[1]

Gene	Forward	Reverse
Human *SHN3*	GCCCTATGTGTGCAAGCACTGT	AGTCCTGGAACAGGTCGTCACT
Mouse *Shn3*	AGAGGCCATTCAGACGAGTGT	CTGCGGAAGCTGAGAGATGT
Mouse *Gapdh*	ACTGAGCAAGAGAGGCCCTA	TATGGGGGTCTGGGATGGAA
Mouse *Actb*	AGGGAAATCGTGCGTGACAT	GAACCGCTCGTTGCCAATAG
Mouse *Lef1*	CCAAGCAAGGCATGTCCAGACACC	GCCTGACAGTGAGGATGGGTAGGG
Mouse *Bglap*	GCAGCACAGGTCCTAAATAG	GGGCAATAAGGTAGTGAACAG
Mouse *Dkk1*	ATCTGTCTGGCTTGCCGAAAGC	GAGGAAAATGGCTGTGGTCAGAG
Human *BGLAP*	AGAGTCCAGCAAAGGTGCAG	TCAGCCAACTCGTCACAGTC
Human *IBSP*	CAACAGCACAGAGGCAGAAA	TTGTGGTGGGGGTTGTAGGTT
Mouse *Axin2*	GCAGATGAACCTGAAGGATACC	TTGATGCCATCTCGTATGTAGG
Mouse *Sost*	CTTCAGGAATGATGCCACAGAGGT	ATCTTTGGCGTCATAGGGATGGTG
Mouse *Hprt*	CTGGTGAAAAGGACCTCTCGAAG	CCAGTTTCACTAATGACACAAACG
Human *HPRT*	GCTATAAATTCTTTGCTGACCTGCTG	AATTACTTTTATGTCCCCTGTTGACTGG
Human *COL1A1*	GATTCCCTGGACCTAAAGGTGC	AGCCTCTCCATCTTTGCCAGCA
Human *AXIN2*	CAAACTTTCGCCAACCGTGGTTG	GGTGCAAAGACATAGCCAGAACC
EGFP	AGCAAAGACCCCAACGAGAA	GGCGGCGGTCACGAA
EGFP-probe	6FAM-CGCGATCACATGGTCCTGCTGG-TAMRA	
(AspSerSer)₆[2]	GATTCATCAGATTCTTCTGATTCATCCGACTCTTCTGACAGTTCAGACAGCTCT	
miR-122[3]/ miR-208a[4]-TS	acaagcttttttgctcgtcttatacaagcttttttgctcgtcttatacaagcttttttgctcgtcttatacaaacaccattgtcacactccaacaaacaccattgtcacactccaacaaacaccattgtcacactcca	
CBA promoter[5]	tctccccatctccccccccctccccacccccaattttgtatttatttattttttaattattttgtgcagcgatgggggcggggggggggggggggggcgcgcgccaggcggggcggggcggggcgaggggcggggcggggcgaggcggagaggtgcggcggcagccaaagcggcgcgctccgaaagtttccttttatggcgaggcggcggcggcggcggccctataaaaagcgaagcgcgcggcgggcggcgggatc	
Lef/Tcf promoter[6]	cgagctcttacgcgagatcaaagggggtaagatcaaagggggtaagatcaaaggggcgcgagatcaaagggggtaagatcaAagggggtaagatcaaagggggtaagatcaaaggggcgcgcccgcgtgctagcccgggctcgagatctagactctagagggtatataatggaagctcgaattccagcttggcattccggtactgttggtaaaaagcttggcattccggtactgttggtaaa	
amiR-33-ctrl (*amiR-ctrl*)	tttgtcttttatttcaggtcccagatctagggctctgcgtttgctccaggtagtccgctgctcccttgggcctgggcccactgacagccctggtgcctctggccggctgcacacctcctggcggggcagctgtgttactgtaggatcgagagggatgttctggcaatacctgtccctctccttactacagtaacacggaggcctgccctgactgcccacggtgccgtggccaaagaggatctaagggcaccgctgagggcctacctaaccatcgtggggaataaggacagtgtcacccctgcaggggatccggtggtggtgcaaatca	
amiR-33-mouse shn3 (*amiR-shn3*)	tttgtcttttatttcaggtcccagatctagggctctgcgtttgctccaggtagtccgctgctcccttgggcctgggcccactgacagccctggtgcctctggccggctgcacacctcctggcggggcagctgtgtacaaactacttgagagcaggtgttctggcaatacctgctgctctgtaatagtttgtacacggaggcctgccctgactgcccacggtgccgtggccaaagaggatctaagggcaccgctgagggcctacctaaccatcgtggggaataagg acagtgtcacccctgcaggggatccggtggtggtgcaaatca	
amiR-33-mouse sost (*amiR-sost*) +	gatctagggctctgcgtttgctccaggtagtccgctgctcccttgggcctgggcccactgacagccctggtgcctctggccggctgcacacctcctggcggggcagctgtgtgacctctgtggcatcattcctgttctggcaatacctgggaatgatcgcgcagaggtcac	

| human amiR-33 -mouse shn3 (hs-*amiR-shn3*) | acggaggcctgccctgactgcccacggtgccgtggccaaagaggatctaagggcaccgctgagggcctacctaaccatcgt gggaataaggacagtgtcacccctgcaggggatccggtggtggtgcaaatcaaagaactgctcctcagtggatgttgcctta cttctaggcctgtacggaagtgttacttctgctctaaaagctgcggaattgtacccgcggccgatccaccggtcgccaccatgggg gcagccttggagtgggttcctgcccctcgggcacacaaacagagctgaagaccaccctgggcacctccttggctggccgca tacctcctggcgggcagctgtgtacaaactacttgagagcaggtgttctggtggtacccacctgctctgtaatagtttgtacacag aggcctgcctggccctcgagagactgccctgactgaaggccctatcaggtgggggaggggatcctgatagagggcactgctg ccactgttggggcccaagaagct |
| Human amiR-33- human shn3 (hs-*amiR-hshn3*)[1] | ggcagccttggagtgggttcctgcccctcgggcacacaaacagagctgaagaccaccctgggcacctccttggctggccgc atacctcctggcgggcagctgtgtttccatggtaagttcaaggctgttctggtggtacccagccttgaagatgccatggaaacac agaggcctgcctggccctcgagagactgccctgactgaaggccctatcaggtgggggaggggatcctgatagagggcactg ctgccactgttggggcccaag |

References

1. Oh, W.-T., Yang, Y.-S., Xie, J., Ma, H., Kim, J.-M., Park, K.-H., Oh, D.S., Park-Min, K.-H., Greenblatt, M.B., and Gao, G. (2023). WNT-modulating gene silencers as a gene therapy for osteoporosis, bone fracture, and critical-sized bone defects. Molecular Therapy *31*, 435-453.

2. Yang, Y.-S., Xie, J., Wang, D., Kim, J.-M., Tai, P.W., Gravallese, E., Gao, G., and Shim, J.-H. (2019). Bone-targeting AAV-mediated silencing of Schnurri-3 prevents bone loss in osteoporosis. Nature Communications *10*, 2958.

3. Chang, J., Nicolas, E., Marks, D., Sander, C., Lerro, A., Buendia, M.A., Xu, C., Mason, W.S., Moloshok, T., and Bort, R. (2004). miR-122, a mammalian liver-specific microRNA, is processed from hcr mRNA and maydownregulate the high affinity cationic amino acid transporter CAT-1. RNA biology *1*, 106-113.

4. Callis, T.E., Pandya, K., Seok, H.Y., Tang, R.-H., Tatsuguchi, M., Huang, Z.-P., Chen, J.-F., Deng, Z., Gunn, B., and Shumate, J. (2009). MicroRNA-208a is a regulator of cardiac hypertrophy and conduction in mice. The Journal of clinical investigation *119*, 2772-2786.

5. Yang, Y.-S., Kim, J.-M., Xie, J., Chaugule, S., Lin, C., Ma, H., Hsiao, E., Hong, J., Chun, H., and Shore, E.M. (2022). Suppression of heterotopic ossification in fibrodysplasia ossificans progressiva using AAV gene delivery. Nature Communications *13*, 6175.

6. Veeman, M.T., Slusarski, D.C., Kaykas, A., Louie, S.H., and Moon, R.T. (2003). Zebrafish prickle, a modulator of noncanonical Wnt/Fz signaling, regulates gastrulation movements. Current biology *13*, 680-685.